

NO-R191 223

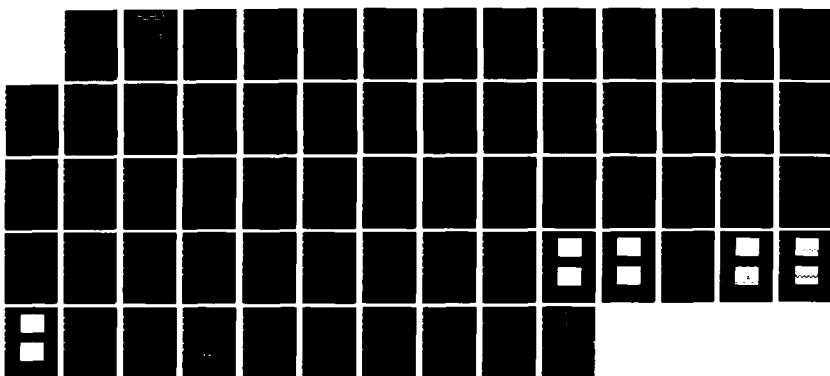
LONG HAUL UNDERWATER FIBER-OPTIC COMMUNICATIONS(U)  
NAVAL POSTGRADUATE SCHOOL MONTEREY CA J G GALLAGHER  
DEC 87

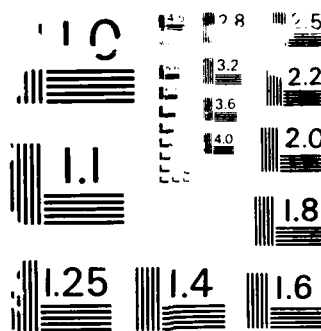
1/1

UNCLASSIFIED

F/G 25/5

NL





REY-DEGON TEST CHART  
NATIONAL BUREAU OF STANDARDS - 921

AD-A191 223

DTIC FILE COPY

(2)

# NAVAL POSTGRADUATE SCHOOL

## Monterey, California



THE

DTIC  
SELECTED  
S D  
MAR 28 1988  
H

LONG HAUL UNDERWATER FIBER-OPTIC  
COMMUNICATIONS

by

John Gregory Gallagher

December 1987

Thesis Advisor:

John P. Powers

Approved for public release; distribution is unlimited.

88 3 28 055

## REPORT DOCUMENTATION PAGE

1a REPORT SECURITY CLASSIFICATION: UNCLASSIFIED		1b RESTRICTIVE MARKINGS	
1c SECURITY CLASSIFICATION AUTHORITY		3 DISTRIBUTION AVAILABILITY OF REPORT: Approved for public release; distribution is unlimited	
1d DECLASSIFICATION/DETERMINATION SCHEDULE		5 MONITORING ORGANIZATION REPORT NUMBER(S)	
1e REPORTING ORGANIZATION REPORT NUMBER(S)		6a NAME OF REPORTING ORGANIZATION: Naval Postgraduate School	
6b OFFICE SYMBOL (if applicable)	6c ADDRESS (City, State and ZIP Code) Monterey, California 93943-5000	7a NAME OF MONITORING ORGANIZATION: Naval Postgraduate School	7b ADDRESS (City, State and ZIP Code) Monterey, California 93943-5000
8a NAME OF FUNDING PROVIDING ORGANIZATION	8b OFFICE SYMBOL (if applicable)	9 PROCUREMENT INSTRUMENT IDENTIFICATION NUMBER	
8c ADDRESS (City, State and ZIP Code)		10 SOURCE OF FUNDING NUMBERS	
		PROGRAM ELEMENT NO	PROJECT NO
		TASK NO	WORK UNIT ACCESSION NO
11 TITLE (Include Security Classification) LONG HAUL UNDERWATER FIBER-OPTIC COMMUNICATIONS			
12 PERSONAL AUTHOR: GALLAGHER, John G.			
13a TYPE OF REPORT: Master's Thesis	13b DATE COVERED FROM 1987 TO	14 DATE OF REPORT (Year, Month, Day) 1987 December	15 PAGE COUNT 63
16 APPROVAL/EXPLANATION			
17 SUBJECT TERMS (Identify by block number)		18 SUBJECT TERMS (Continue on reverse if necessary and identify by block number) Fiber-optics, Lasers, Fiber-optic cable, Optical transmitters, Laser Driver Circuits	
19 ABSTRACT (Continue on reverse if necessary and identify by block number) The subject of this thesis is the design, construction and testing of a long haul fiber-optic communication system. This system would remotely monitor the voltage of a one volt, one ampere long-life saltwater battery at nominal depths of 1000 meters. It is the continuation of an ongoing project to monitor the battery in its deployed deepwater environment. The goal was to find methods to increase the transmission distance of the previous short haul (less than 10 kilometers) communication link to greater than 30 kilometers by utilizing a laser source instead of an LED and single mode fiber-optic cable instead of multimode cable. Additionally the capability to monitor various other environmental or system parameters by the use of a microprocessor.			
20 DETERMINATION AVAILABILITY OF ABSTRACT <input checked="" type="checkbox"/> SAME AS REPORT <input type="checkbox"/> DIFFERENT		21 ABSTRACT SECURITY CLASSIFICATION UNCLASSIFIED	
22b TELEPHONE (Include Area Code) POWERS, J. P. (408) 646-2082		22c OFFICE SYMBOL 62Po	

Approved for public release; distribution is unlimited

Long Haul Underwater Fiber-Optic Communications

by

John Gregory Gallagher  
Lieutenant, United States Navy  
B.S.B., North Texas State University, 1979

Submitted in partial fulfillment of the  
requirements for the degree of

MASTER OF SCIENCE IN ELECTRICAL ENGINEERING

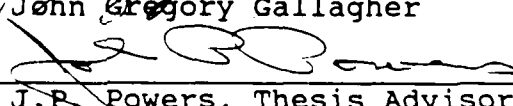
from the

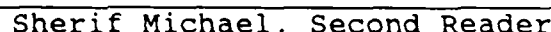
NAVAL POSTGRADUATE SCHOOL  
December 1987

Author:

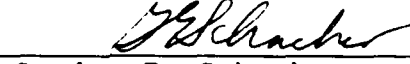
  
John Gregory Gallagher

Approved by:

  
J.P. Powers, Thesis Advisor

  
Sherif Michael, Second Reader

  
J.P. Powers, Chairman Department  
of Electrical and Computer Engineering

  
Gordon E. Schacher  
Dean of Science and Engineering

## ABSTRACT

The subject of this thesis is the design, construction and testing of a long haul fiber-optic communication system. This system would remotely monitor the voltage of a one volt, one ampere long-life saltwater battery at nominal depths of 1000 meters. It is the continuation of an ongoing project to monitor the battery in its deployed deepwater environment. The goal was to find methods to increase the transmission distance of the previous short haul (less than 10 kilometers) communication link to greater than 30 kilometers by utilizing a laser source instead of an LED and single mode fiber-optic cable instead of multimode cable. Additionally the capability to monitor various other environmental or system parameters by the use of a microprocessor.



Accession For	
NTIS GRA&I	<input checked="" type="checkbox"/>
DTIC TAB	<input type="checkbox"/>
Unannounced	<input type="checkbox"/>
Justification	
By _____	
Distribution/	
Availability/	
Dist Spec	
A-1	

## TABLE OF CONTENTS

I.	INTRODUCTION.....	9
A.	BACKGROUND.....	9
II.	SYSTEM OVERVIEW.....	13
A.	SYSTEM DESCRIPTION.....	13
B.	LIGHT SOURCES.....	15
1.	Diode Laser vs. LED.....	15
2.	Diode Laser vs. LED.....	19
C.	FIBER-OPTIC LINK.....	20
1.	Attenuation.....	21
2.	Single vs. Multi-mode Fiber.....	21
3.	Couplers and Splice Techniques.....	23
4.	System Losses and Power Budget.....	26
D.	TRANSMITTER SYSTEM.....	28
1.	Design Parameters.....	29
2.	Voltage to Frequency Converter(V/F Converter) ..	30
3.	Driver System.....	32
a.	Sharp CD Laser Driver ICs.....	33
b.	Slow Start Driver.....	37
c.	Driver Comparisons and Results.....	40
E.	MICROPROCESSOR CONTROL AND CIRCUIT.....	41
1.	NSC800 Microprocessor.....	41
2.	MM58167 Microprocessor Real Time Clock (RTC) ..	43

3. Controller Circuit.....	44
III. TEST AND EVALUATION.....	47
A. TRANSMISSION DISTANCE IMPROVEMENT.....	47
B. TRANSMISSION BANDWIDTH.....	51
IV. CONCLUSIONS AND RECOMMENDATIONS.....	55
APPENDIX A: (LASERTRON DIODE LASER SPECIFICATION SHEETS) .....	56
LIST OF REFERENCES.....	59
BIBLIOGRAPHY.....	61
INITIAL DISTRIBUTION LIST.....	62

## LIST OF TABLES

1. DATA TRANSMISSION RATES AND COUPLED POWER.....	19
2. LOSS CHARACTERISTICS SINGLE VS. MULTI-MODE FIBER.....	27
3. POWER CONSUMPTION COMPARISON IN MILLIWATTS.....	40

## LIST OF FIGURES

1.1	Original System Diagram.....	11
1.2	Desired System Diagram.....	12
2.1(a)	Attenuation Losses Over Distance.....	22
2.1(b)	Losses vs. Wavelength in Single Mode Fiber.....	22
2.2	Single Mode and Multimode Geometry.....	24
2.3	Delay Dispersion in a Fiber.....	24
2.4	Voltage-to-Frequency Converter Circuit.....	31
2.5(a)	Sharp Laser Driver IC Chip IR3C01/N.....	34
2.5(b)	Sharp Laser Driver IC Chip IR3C02/N.....	34
2.6	Sharp IR3C01/N Diode Laser Driver Circuit.....	36
2.7	Slow Start Diode Laser Driver Circuit.....	38
2.8	NSC800 Microprocessor Circuitry.....	42
2.9	Real Time Clock Power and Sleep Circuitry.....	46
3.1	10 KHz Signal After 41 Kilometers.....	49
3.2	512 Hz Signal After 41 Kilometers.....	49
3.3	700 Hz Signal After 41 Kilometers.....	50
3.4	280 Hz Signal After 71 Kilometers.....	50
3.5	100 KHz Signal After 10898 Meters.....	52
3.6	150 KHz Signal After 10898 Meters.....	52
3.7	500 KHz Signal After 10898 Meters.....	53
3.8	1.1 MHz Signal After 10898 Meters.....	53
3.9	12 MHz Signal After 10898 Meters.....	54
3.10	12 MHz Signal After 10898 Meters.....	54

#### ACKNOWLEDGMENT

I would like to take this opportunity to acknowledge and thank Mr. John Glenn, the Electroptics Lab Manager, for all the expert assistance and encouragement he gave me during work on this thesis.

## I. INTRODUCTION

The subject of this thesis is the design, construction and testing of a long haul fiber-optic communication system. This system would remotely monitor the voltage of a one volt, one ampere long-life saltwater battery at nominal depths of 1000 meters. It is the continuation of an ongoing project to monitor the battery in its deployed deepwater environment. The goal was to find methods to increase the transmission distance of the previous short haul (less than 10 kilometers) communication link [Ref. 1, 2] to greater than 30 kilometers by utilizing a laser source instead of an LED and single mode fiber-optic cable instead of multimode cable. Additionally, the capability to monitor various other environmental or system parameters has been incorporated by the use of a microprocessor.

### A. BACKGROUND

The field of fiber-optic communications is continually expanding. The reasons for this expansion are the advantages associated with fiber-optics, such as greater transmission bandwidth and increased data transmission rates, and distances. Also there are the improved reliability, maintainability, and reduction of system power improvements available with today's optical fiber systems.

Systems to meet the requirement for a one-way sea-to-shore

remote monitor system have been previously studied at the Naval Postgraduate School. Koo [Ref. 1] designed and tested a system that could transmit a signal representing the voltage of a test battery through an optical fiber in the laboratory. Later, Gibson [Ref. 2] successfully modified, tested, and deployed Koo's fiber-optic system underwater and achieved transmission data distances of 1.5 kilometers using a light emitting diode (LED) and multi-mode fiber-optic cable. Figure 1.1 is an illustration of that system and is shown as it would appear in its deployed configuration. The improved version of this system that is desired is illustrated in Figure 1.2.

Chapter II gives some background on semiconductor lasers and explains optical fiber properties. The details of the transmission system, the improvements and specifications, the microprocessor controller, and the rational for those choices are also in chapter II. Chapter III covers the system testing and evaluation, and finally chapter IV contains the conclusions and recommendations.

This thesis addresses the improvement of the data transmission distance in a laboratory setting only; actual deployment is scheduled for follow-on efforts by other students.

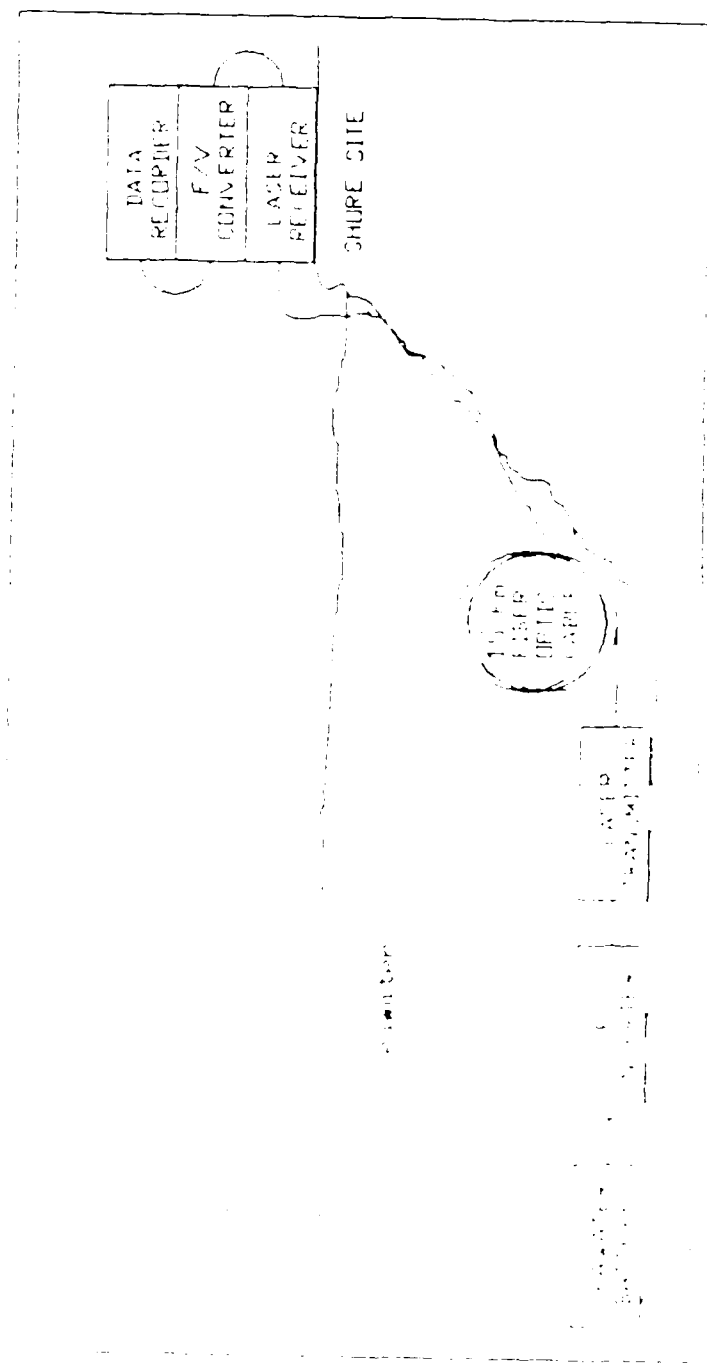


Figure 1.1 Original System Diagram

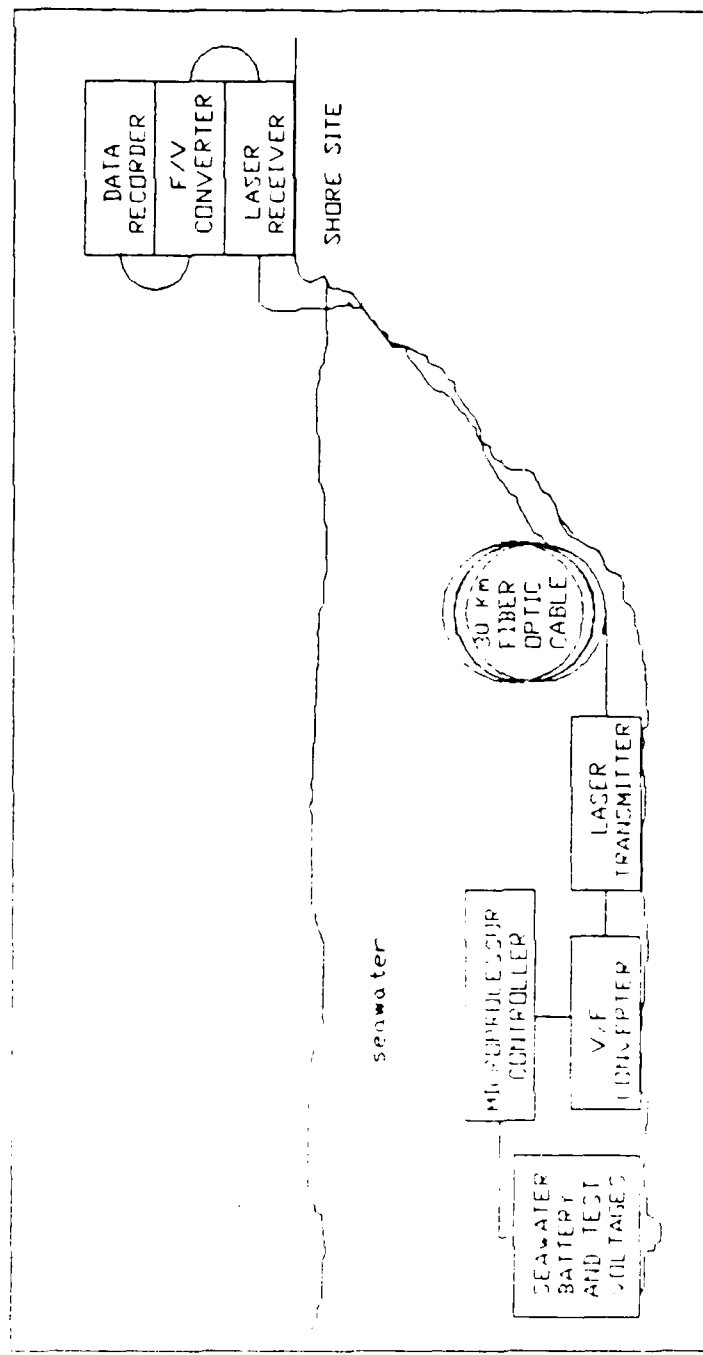


Figure 1.2 Desired System Diagram

## II. SYSTEM OVERVIEW

The long haul communication system of Figure 1.2 consists of five subsystems or sections. They are the desired parameters to be measured (e.g., the test battery voltage and/or environmental parameters such as current velocity, temperature, salinity, etc.), the transmitter microprocessor controller, the voltage-to-frequency converter circuitry, laser driver and source circuitry, and the fiber transmission medium. This chapter will discuss each section with the exception of the battery, in greater detail. In order to understand laser communication systems some general background in semiconductor lasers and optical fiber parameters is helpful. The following sections will attempt to give that information.

### A. SYSTEM DESCRIPTION

The goal of the system is to transmit measured data at predetermined programmed measurement intervals (e.g., fifteen minutes). This is done by first converting the measured voltage ( $V_{in}$ ) into a square wave whose frequency ( $f_{out}$ ) is derived from the following:

$$f_{out} = V_{in} * 10000 \text{ Hz/V} \quad (2.1)$$

The square wave voltage is converted into an optical replica by the source and transmitted through the fiber. The received optical signal is converted to a voltage by the receiver and

fed to a frequency-to-voltage converter that reconstructs (ideally) the measured voltage (or a scaled replica). This voltage is sampled and stored by the computer recorder.

In order to understand this monitoring system the transmission of a test voltage (the battery voltage or the output of a device measuring one of the environmental parameters) will be traced through one cycle from system turn ON to turn OFF.

Prior to the system coming ON, the power bus of the system is not connected to the circuit until the clock circuit of the microprocessor counts down the programmed fifteen minute interval between transmissions. Once this time has elapsed the circuit awakes and the microprocessor runs a program held in the EPROM. The program controls the CD4066E IC switch. This switch cycles through the various test voltages which in turn are applied to the input of the voltage-to-frequency converter circuit. The voltages are converted to representative frequencies (e.g., a one volt measurement on the test battery will be converted to 10 KHz signal). This signal will be used to modulate the output of the current driver circuit that operates a 1300 nm diode laser. Each test voltage in turn will then be multiplexed into the driver circuit. The diode laser's output is carried on single mode fiber to a detector circuit located ashore.

## B. LIGHT SOURCES

The invention of the laser and its marriage to fiber optics has expanded the technology of communications. The capabilities of fiber communications now far exceed those of the twisted wire pair and coaxial cable. There are many different optical sources; these include ruby, rare gas, certain foods and solid state or semiconductor lasers. In particular, the semiconductor laser has emerged after two decades of research as perhaps the most important component in fiber-optic systems. The classes of semiconductor sources used in optoelectronic communications are the light emitting diode (LED) and injection laser diode (ILD) (or simply the diode laser). Further classification of these sources is made by their wavelength. Short wavelength sources operate at a wavelength in the 500 to 1000 nm range while long wavelength sources operate at a wavelength in the range extending from 1200 to 1600 nm. The differences between diode lasers and LEDs will be explored in the following sections.

[Ref. 3:pp. 46-47, 4:p. 4-1]

### 1. Diode Laser vs. LED

Semiconductor optical sources use the basic forward biased p-n junction physics of semiconductor devices along with quantum electronic concepts common to all lasers. The semiconductor source, compared to the HeNe gas or the Nd-doped YAG solid state laser offers a much smaller package, potentially lower costs and power consumption, plus the

ability to modulate the output up to Gigahertz (GHz) rates by simply modulating the current passing through the device [Ref. 5:p. 1].

The diode laser and the light emitting diode (LED) are related since they are both solid state junction devices. These semiconductor sources are fabricated by growing adjacent layers of semiconductor material using the various processes of epitaxial technology. By growing the devices in layers the desired wavelength is obtainable by precisely selecting the dopant amounts and type of semiconductor material. The finished laser devices are made up of materials such as GaAs, AlGaAs, and InGaAsP to name a few. Two and three element semiconductor lasers combine to make short wavelength devices, while the four element ones make up the longer wavelength sources.

Despite their similarities the LED has a broader spectral lineshape and less directional emissions, also its modulation capabilities are more limited compared to the diode laser. The main cause for this difference lies in the respective device geometry. Surface and edge emitters are two of the structures used for obtaining maximum radiance in LEDs [Ref. 5:p.486]. Although LEDs are excellent sources for short distance fiber communications, they do not make a good choice for long haul fiber communication systems. The main reason for this is that LEDs have a beam divergence that is much greater than a diode laser and their radiance or optical power

output is orders of magnitude less. For instance at 1300 nm an LED source has an output power of -20 decibels below a milliwatt (dBm) while a diode laser at the same wavelength is 0 dBm. This difference could mean a difference of 20 Km at a fiber attenuation of 1.0 dB/Km, a very conservative estimate of attenuation at 1300 nm.

There are several structural techniques used with diode lasers to obtain narrower wavelengths and greater output power. One of these is the index guided laser; it has a very flat and narrow junction area to confine the charge carriers and reflective coatings on the parallel ends of the junction area. One face is usually coated with a 100% reflecting surface so to produce light output at the opposite face only. This parallel type of construction acts as an optical resonator thereby functioning as a Fabry-Perot interferometer resonator. Another type of diode laser construction, the distributed feedback laser, uses an internal corrugated surface at the interface of two active layers of the semiconductor surface. The periodicity of the corrugated facet is etched to match the desired wavelength and acts to selectively couple the forward and backward propagating waves by means of backward Bragg scattering. This in turn produces much purer output at extremely narrow frequencies.

[Ref. 4:pp. 4-13,15, 6:pp. 287-9]

The emissions of the diode laser are similar to those of the LED below a critical point called laser threshold,

( $I_{th}$ ). That is, the diode laser operating below threshold emits light as an LED does: continually, spontaneously and randomly. The diode laser begins spontaneous emission as soon as current is applied but its output is non-coherent light. Once this current threshold level is met, the semiconductor laser starts lasing by stimulated emission and emits the coherent light associated with such devices. The reason for this is that, prior to threshold, the weak stimulated emission has to compete against the absorption processes during which an electron-hole pair is generated at the expense of an absorbed photon. Since the electron population in the valence region band generally far exceeds that of the conduction band, absorption dominates. At the threshold of the external current, a sufficient number of electrons are present in the conduction band to make the semiconductor optically transparent. With a further increase in current, the active region of the semiconductor laser exhibits optical gain and can amplify the electromagnetic radiation passing through it.

[Ref. 6:pp. 14-15]

In most cases longer wavelength diode laser sources are favored in optical communication systems because of the decreased dispersion or lower losses that occur at these wavelengths. These lasers have increased spectral purity and greater radiance than LEDs. Table I shows some of the differences in the radiance of LED versus lasers and their data transmission rates.

TABLE 1  
DATA TRANSMISSION RATES AND COUPLED POWER

<u>Short Wavelength</u> 820 nm		
Transmission Rates	<u>LED</u>	<u>Laser</u>
	150 Mb/s-km	25 Gb/s-km
Source Power		
	-30 dBm	0.0 dBm
<u>Long Wavelength</u> 1300 nm		
Transmission Rates	<u>LED</u>	<u>Laser</u>
	1.5 Gb/s-km	25 Gb/s-km
Source Power		
	-20 dBm	0.0 dBm

All of the available information pointed to the advantages of long wavelength laser diode sources over LEDs for their increased data transmission distance. Therefore the Lasertron QLM-1300SM-BH 1300 nm laser diode was selected to replace the LED source of the original system. The next section is a description of the chosen source.

## 2. Lasertron Diode Laser

The Lasertron Inc. QLM-1300-SM-BH is a GaInAsP buried heterostructure laser capable of 1 mW coupled output power. The laser module has a low current thermoelectric cooler, a high performance GaInAs monitor photodiode, and a precision thermistor incorporated in a single small package. The cooler provides constant temperature operation of the diode chip,

removing thermal variations that can cause significant changes in the output power. The photodiode monitor can be used to monitor the outward going light for proper modulation or for temperature and/or aging effects on the power level. The thermistor is used to sense the laser operating temperature and its output is used in a feedback circuit to control the thermoelectric cooler. Included with the laser diode is a Corning single mode fiber attached to the laser using a taper and lens coupling scheme to provide minimum optical feedback to the laser element and improve the coupling efficiency. The center wavelength of 1290 nm takes advantage of the typical zero dispersion wavelength (near 1300 nm) of conventional single mode fiber. (For a more in depth description of dispersion and fiber parameters in general see section 2.C.1.) The narrow spectral width, tight wavelength tolerance and high coupled power make this module a good choice of source for long distance telecommunication applications. Specification sheets concerning Lasertron Lasers is contained in the Appendix.

#### C. FIBER-OPTIC LINK

Some of the many advantages of using fiber-optic links include light weight, immunity from EMI, lack of crosstalk, no sparking hazard, and low cost. This portion of the chapter will discuss fiber-optic links covering attenuation, the differences between single and multi-mode fiber, connectors, splicing techniques, and system losses.

## 1. Attenuation

The most important of the characteristics of fiber is attenuation. Attenuation is the loss of light power or energy as the light propagates down a length of fiber as illustrated in Figure 2.1(a). Absorption and scattering are the two mechanisms by which this loss can occur. In absorption, the light interacts with impurities in the fiber or with the silica glass itself at some wavelengths to cause the transitions of the electrons [Ref. 3:pp. 11] losing energy in the process. These electrons then can loose their energy as heat from the mechanical vibrations or by emitting light at other wavelengths. The other type of attenuation by scattering is caused when atoms, impurities, or geometrical imperfections in the fiber redirect the light out of the forward direction. Figure 2.1(b) shows the losses in a single mode fiber as a function of wavelength.

In the early stages of fiber technology the average attenuation losses of 20 dB/Km were mostly due to absorption by impurities in the glass. Today the standard for single mode fiber attenuation losses is around 0.5 dB/Km at 1300 nm.

## 2. Single vs. Multi-mode Fiber

As already mentioned the fiber consists of a core and cladding region, the core typically has a diameter of between 5 um and 100 um. The small core fiber known as a single mode fiber propagates light differently than that of the larger core (multi-mode) fiber. "Small" in single mode fibers means

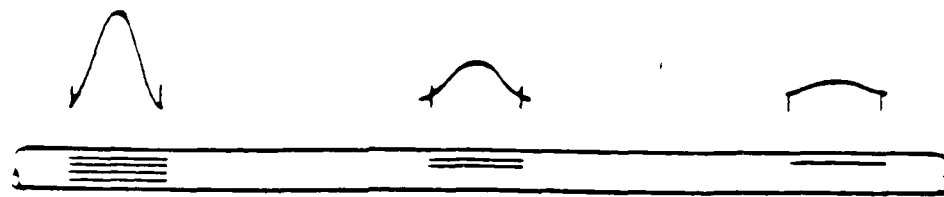


Figure 2.1(a). Attenuation Losses Over Distance  
(From Reference 3)

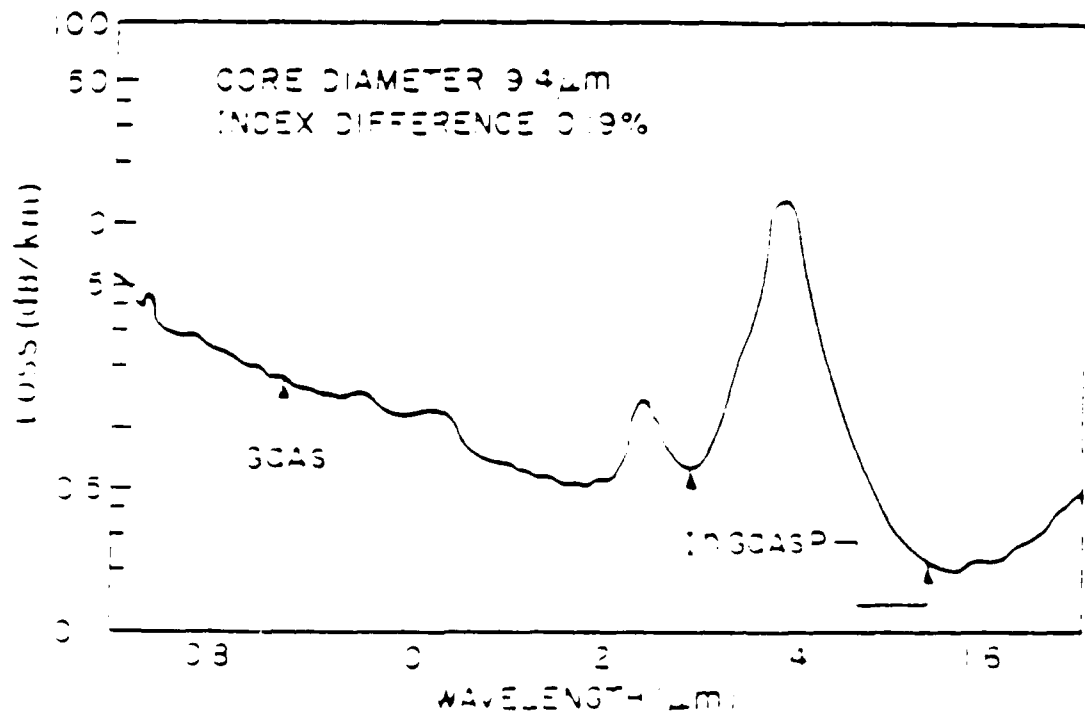


Figure 2.1(b). Attenuation Losses in Single Mode Fiber as a Function of Wavelength (From Reference 6)

small with respect to the wavelength carried, typically the core is only a few times larger than the wavelength. Thus "large" corresponds to a core size that can range from tens to even hundreds of times greater than the wavelength carried Figure 2.2.

As a pulse of optical energy travels along a fiber it can spread out in time as shown in Figure 2.3. This delay distortion is called dispersion. There are two types of dispersion: modal pulse delay distortion and material dispersion. One way to combat the problem of modal dispersion is to use graded index fibers, i.e., fibers that have an increasing optical density toward the center of the core. Another method is to use single mode fiber, in these fibers the diameter is so small that only one electromagnetic mode can exist. Two methods exist to minimize the material dispersion. The first is to operate at 1300 nm where the material dispersion is canceled by the waveguide dispersion, leaving a minimum in the net dispersion. The second method is to use a source with minimum linewidth since the material dispersion is proportional to the source linewidth.

[Ref. 3:pp. 12-19]

### 3. Couplers and Splice Techniques

Seldom do fibers come in the exact length necessary to do the job. At the location considered for deployment the 1000 m desired depth requires a cable length of 30 km to comfortably reach from the deployed location to shore. Since

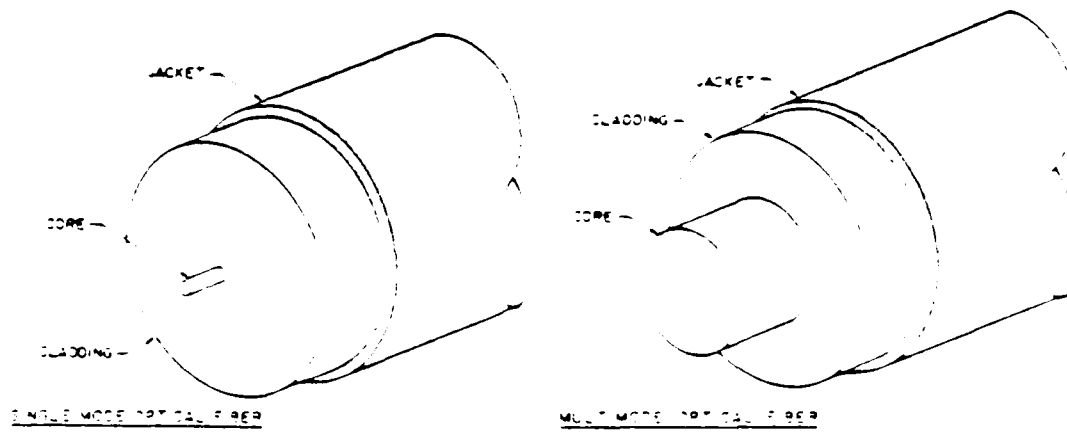


Figure 2.2 Single Mode and Multi-mode Geometry  
(From Reference 3)

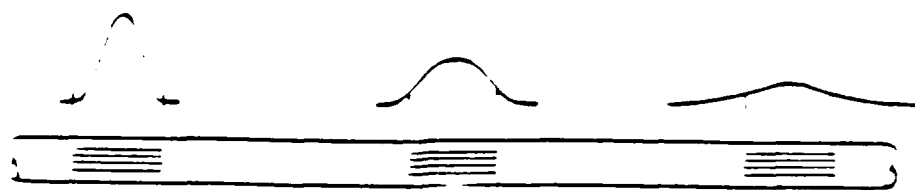


Figure 2.3 Delay Dispersion in a Fiber  
(From Reference 3)

it would be nearly impossible to find a single 30 Km piece of fiber, a method of connecting the pieces is necessary. These connections need have low losses (insertion losses) associated with them, have high strength and be simple to install. There are two methods of joining fibers available: splicing and connectors. A splice is a permanent joint of two fibers; connectors can be joined and removed repetitively.

There are numerous kinds of connectors available for use with optical fiber, some are: SMA, ST, Biconic, or BNC. Each type uses a different fiber alignment and cable coupling method. Unfortunately there is no standard connector type, although SMA, ST, and Biconic are enjoying wide industry use at this time. The insertion losses with connectors can range from a few 0.1s to a few dB of attenuation. Even though connectors can be joined and removed the connector itself must be permanently attached to the end of a fiber. [Ref. 4]

Permanent splices can be made in a number of ways. Fusion splicing machines, for instance, join the two fiber ends by heating and then fusing them together and are capable of making splices with less than 0.1 dB/splice loss. A recent improvement on the V-groove method of splicing [Ref. 4] by Photodyne Inc. is their Fiber Splicer Kit that can be accomplished easily and quickly (less than two minutes) under field conditions. The losses using this method are comparable to fusion splicing. Within all these methods of joining fibers there are many different factors intrinsic and

extrinsic that determine the coupling efficiency.

#### 4. System Losses and Power Budget

The knowledge of types of losses that occur in fiber-optic systems is necessary in power budget computations.

These calculations are important to determine if the communication system will be able to overcome the total losses and be detected at its terminus. Knowing what power is available from the source,  $P_T$ , that can be launched into the fiber and the minimum detectable power of the receiver,  $P_R$ , the allowable total amount of losses in dB can be calculated from

$$\text{Losses (dB)} = 10 \log (P_T/P_R) \quad (2.2)$$

The combination of the losses from attenuation and splices along with a few others to be mentioned make up part of a system power budget. It is possible to try different combinations of losses in order to improve the overall power budget. This includes replacing components or switching to single mode fiber from multi-mode. Table II lists some the typical conservative values of the loss parameters associated with fibers in optical communication systems.

TABLE 2  
AVERAGE LOSS CHARACTERISTICS IN dB FOR  
SINGLE VS. MULTI-MODE FIBER

	<u>Multi-mode</u> @ 820 nm	<u>Single Mode</u> @ 1300 nm
Attenuation - $a_0$	2.5 dB/Km	0.6 dB/Km
Coupling - $l_C$	1.5 per	1.5 per
Splice - $l_S$	0.5 per	0.5 per
Aging - $l_A$	-6 dB	-6 dB

The power budget equation can also be written using the terms for the losses of Table II as follows;

$$10\log(P_T/P_R) = a_0 L + l_T + n l_S/C + l_R + l_A + l_M \quad (2.3)$$

where L equals the length of the fiber cable,  $l_T$  is the transmitter to fiber loss, n the number of splices or couplers,  $l_R$  the fiber to receiver losses, and finally  $l_M$  is the system margin. As long as the system margin is positive the link should work properly.

The aim of this thesis was to attain at least 30 Km transmission distance. The maximum losses the system could stand were calculated using equation 2.5. The detector is capable of responding to optical signals of -40 dBm (0.1 uW) or greater, and the diode laser has a rated power output of 0 dBm (1 mW). Using equation 2.4 and substituting in the power values below

$$10 \log (1.0 \text{mW} / 0.1 \mu\text{W}) = 40 \text{ dB} \quad (2.2)$$

This means the system can stand any combination of losses totaling no more than 40 dB attenuation. Using the average losses from Table II for thirty kilometers of cable, and computing for both multi-mode and single mode fibers at attenuations of 2.5 and 0.6 dB/Km result in 75 and 18 dB respectively. It can be seen that the single mode fiber was the only way to achieve the desired distance. Subtracting the 18 dB from the initial system 40 dB leaves 22 dB for the other loss sources. Allowing for the other losses such as the 6 dB aging loss, another 6 dB for  $l_T$  and  $l_R$  together, eight splices for 4 dB, and finally two connectors at 3 dB each leaves us with no system margin. A system made up of these type and number of components should be received after 30 Km. By carefully working with the components small gains can be made and a larger system margin can be obtained. For example the single mode fiber used in this project had measured losses of actually 0.53 dB/Km, so at 30 Km this gives 15.9 dB loss for the first term in equation 2.5. This one change alone leaves us 2.1 dB of system margin. As is readily apparent by the calculations and the characteristics of Table II, single mode systems have much in their favor to warrant their use.

#### D. TRANSMITTER SYSTEM

The general requirements of the system, cost, and availability of parts were the driving factors in determining components. This section discusses the design parameters, the

voltage to frequency converter, and the driver subsection. Also where applicable the basic differences between the two systems.

### 1. Design Parameters

The original design specifications of this system required it to monitor the voltage of a prototype saltwater battery. Koo [Ref. 1] built a fiber-optic communication system capable of optical digital transmission of the voltage of a test battery. Later, Gibson [Ref. 2] was able to deploy an improved version of this system and monitor a test battery's voltage from a shore site. His system was able to successfully transmit through 1.5 kilometers of fiber. Although both these systems were very good, they are not capable of transmitting the information through the desired 30 kilometers of fiber. (This requirement was added after Gibson's work. Prior to the decision to deploy the battery at 1000 m depth, the assumed operating depths and site-to-shore distances were much shorter.)

In addition to the original requirement of monitoring the seawater battery voltage, this thesis includes the capability of the system to monitor more than a single voltage (i.e., the ability to monitor the battery and one or more other system or environmental factors). In light of the new capability the author was faced with two choices: the construction of a bi-directional communication link or the installation of some sort of controller at the transmission

end of the system.

The engineering factors necessary for a bi-directional link would be quite arduous to implement. This type of system would required two laser sources and detectors operating at different wavelengths, optical splitters, or two separate fiber systems and all the associated circuitry. The cost of such a system would easily exceed twice the amount for a single direction system, not to mention the problems associated with two systems. With these difficulties in mind the decision was made to maintain the original design and utilize a microprocessor to control the transmitter circuitry. This controller is described in section E of this chapter.

## 2. Voltage to Frequency Converter (V/F Converter)

Communication transmissions through fiber are optimized for digital signals of TTL logic [Ref. 7]. The circuit of Figure 2.4 uses an LM331 voltage-to-frequency converter that converts a 1 to 10 volt dc voltage to a corresponding 1 KHz to 10 KHz TTL signal. Since the voltage of the battery under test is only a one volt, the input voltage must be prescaled or amplified in order to use the LM331 properly. Gibson [Ref. 2:p. 11] used an LM124J operational amplifier to prescale the voltage of the battery under test by a factor of ten prior to feeding it into the V/F converter. In this manner the amplified one volt input signal voltage will match the input range of the LM331 and follow with a linear frequency dependence, as the test voltage

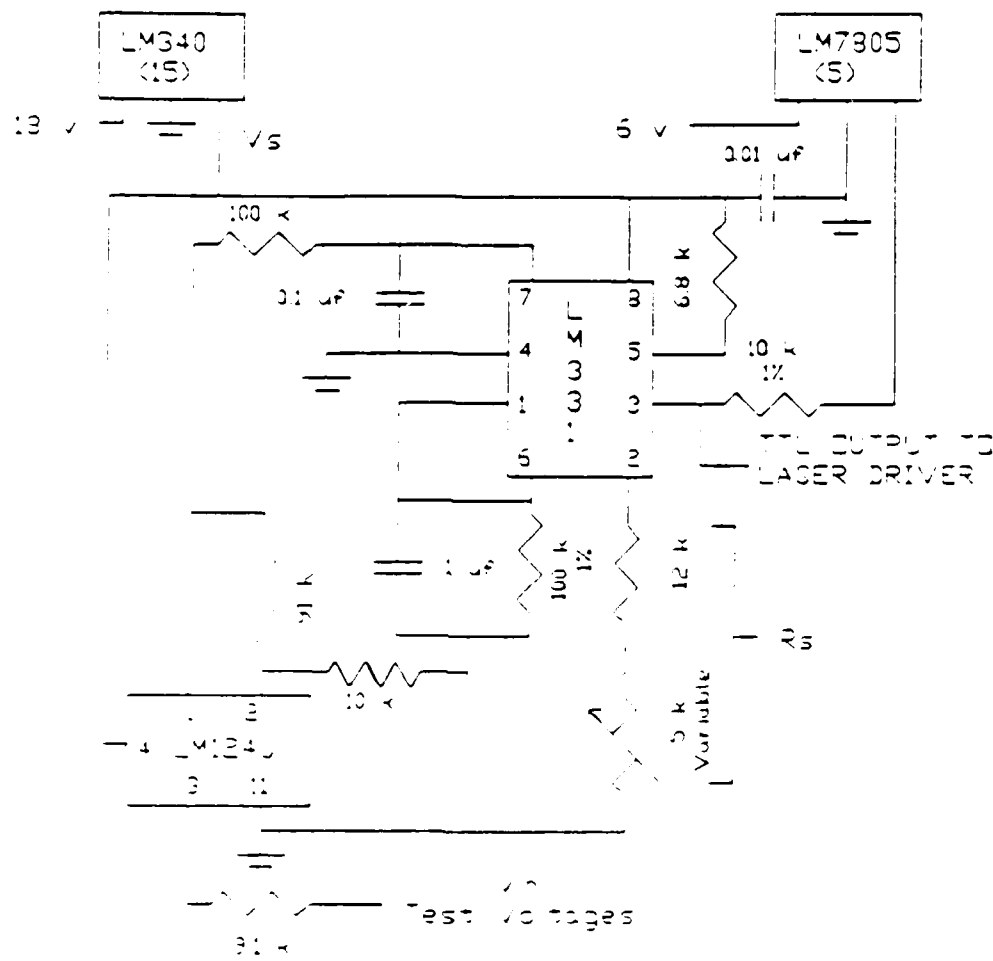


Figure 2.4 Voltage-to-Frequency Converter Circuit  
(From Reference 1)

changes. The linearity of the LM331 output as compared to the input is  $\pm 3$  percent. The relationship of the frequency of the output of the LM331 to the saltwater battery or test voltages is given by the equation,

$$f_{\text{out}} = 10V_{\text{in}}R_s/2.09V_{\text{cc}}R_lR_tC_t \quad (2.4)$$

where  $f_{\text{out}}$  is the output frequency of the V/F converter;  $V_{\text{in}}$  is the battery or other parameter test voltage;  $V_{\text{cc}}$  the supply voltage (5 volts dc);  $R_s$ ,  $R_l$  and  $R_t$  are the source, load, and timing resistances respectively; and  $C_t$  is the timing capacitance.

### 3. Driver System

The output TTL signal of the V/F converter was fed into a SN75451 Dual Peripheral Positive AND Driver. This IC modulated an inexpensive 820 nanometer Hewlett Packard HFBR 1404 LED in Gibson's system. Since the goal of this thesis was to incorporate a laser diode as the source of the system instead of the original LED, the driver circuit needed to be altered. Interest was initially directed at the Sharp Compact Disk (CD) Laser Driver (IR3C0XX series) Integrated Circuit chip. These ICs are used in Compact and Video Disk Players as the current-controlling driver for the laser diode. For proper CD player operation it is necessary that the output of the laser diode be constant because the information on the disk is read by the amount of light reflected back from the disk. This binary information, ZEROS and ONES, is encoded by a series of pits (ZEROS) and reflective areas (ONES) on the

surface of the disk. Light striking a pit will be diffused and not recorded on the detector while conversely the light striking a flat reflective area all be returned to the detector. Thus it is important that the output of the diode laser be maintained at the optimum level for reading the laser disks.

The feasibility of using one of these drivers as a source driver in our application was studied. The obvious benefits of using one of these ICs would be that only one inexpensive IC chip need be added to the original V/F circuitry. The next sections describe the research directions followed.

#### a. Sharp CD Laser Driver ICs

The Sharp Electronics Corporation fabricated several driver ICs for use in laser driver applications. In particular, the IR3C01/N and the IR3C02/N (Figure 2.5) compact disk player source driver ICs were studied for their applicability to this problem. Both of the ICs were designed as a basic constant current source for the laser diode, also automatic power controllers were incorporated to compensate for the output power fluctuations of the diode laser with changes in the temperature and age. The output power is maintained by a feedback loop from the monitor output pin to the laser diode input. An external control input to the IC is available to switch the circuit on and off using a TTL voltage input. It was originally assumed that the easiest and best way of modulating the output of the diode laser would be by

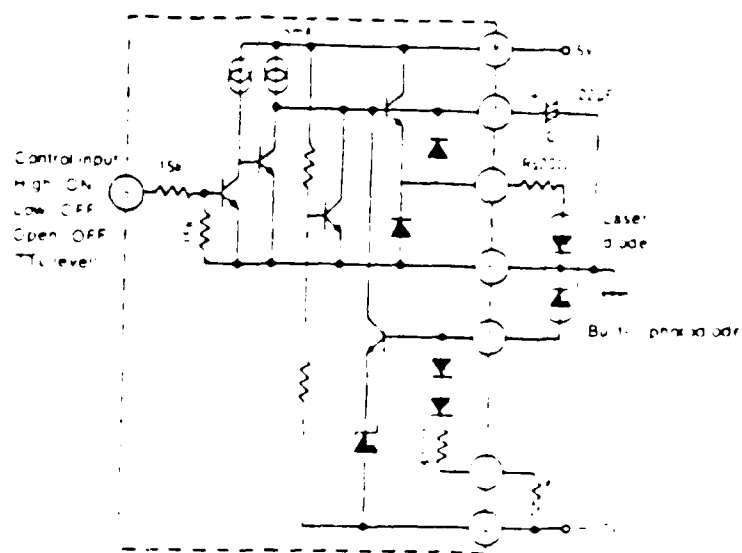


Figure 2.5(a) Sharp Laser Driver IC IR3C01/N  
(From Reference 8)

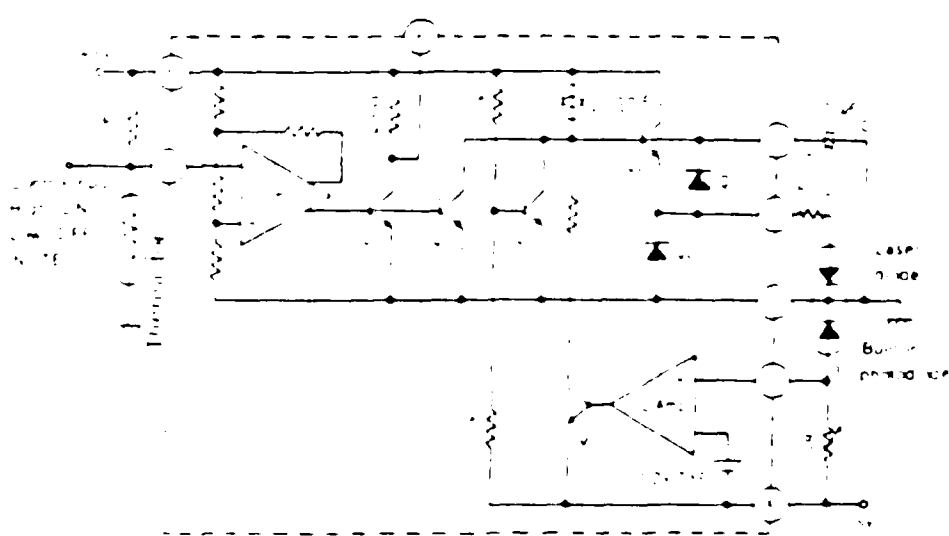


Figure 2.5(b) Sharp Laser Driver IC IR3C02 N  
(From Reference 8)

coupling the output of the V/F converter to the Sharp's external control input pin. This method proved successful but the diode laser drive current was subjected to swings from zero to  $I_{MAX}$ . This was because the control input pin acts as a switch and there is no way to moderate these current excursions using the internal circuitry of the driver chip. The control input turns the circuitry ON or OFF. Since laser diodes are somewhat fragile instruments, operation under conditions such as these would not continue very long before the laser diode failed due to the rapid temperature changes that follow the current excursions.

However the IR3C01/N IC chip can be modified externally by use of some resistors and a transistor to regulate the current through the diode laser source as shown in Figure 2.6 [Ref. 8:p. 28]. The desired method of current modulation would be to keep the current in the diode laser at or just below threshold ( $I_{th}$ ) until necessary. In this way the diode laser will still be on and barely emitting light at threshold but the power output will not be enough to be detected at the receive end of the communication circuit. Therefore to provide the maximum power output of the source ( $I_{MAX}$ ) the current change required ( $I_{th}$  to  $I_{MAX}$ ) would not be as great as the excursions of the previous system (0 to  $I_{MAX}$ ). The difference between threshold and maximum power output is 10 mA for the particular diode laser used, a value not uncommon to other sources of this type.

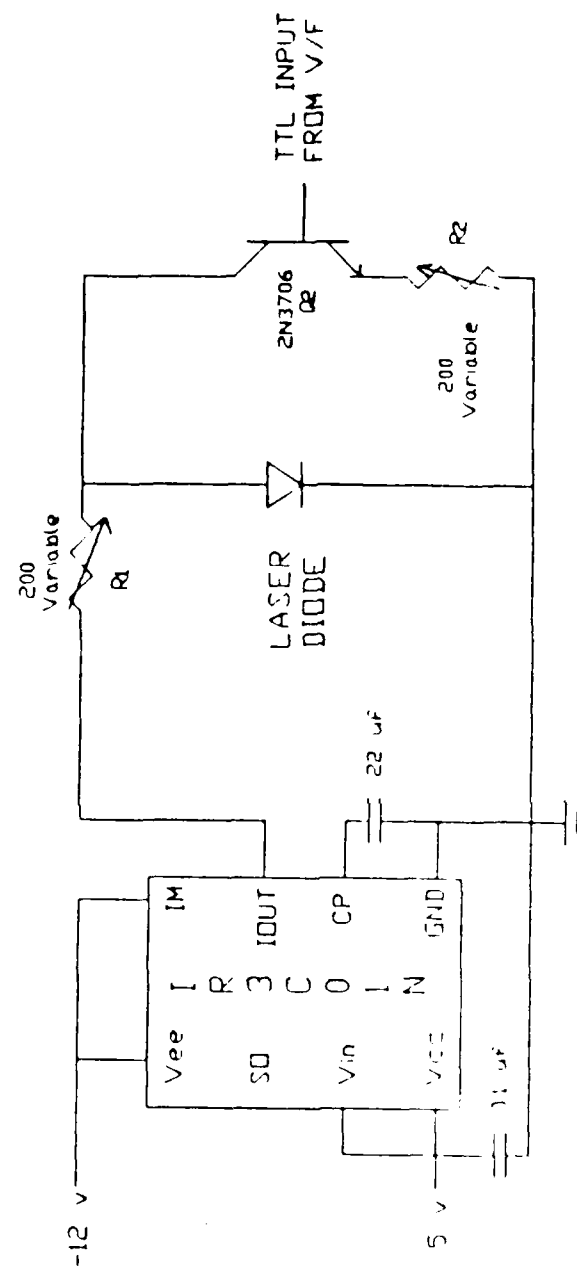


Figure 2.6 Sharp IR3COIN Diode Laser Driver Circuit

The IR3C01 requires +5 and -12 volts to operate. This necessitated the incorporation of a 12 volt negative power supply to be added to the original system with the resulting extra power draw on the 18 volt battery bus. It was decided that another method might simplify the design problem.

b. Slow Start Driver

Although the Sharp CD driver did an excellent job, the power considerations dictated the use of the more traditional laser driver made of discrete components. The circuit of Figure 2.7 illustrates this method using a simple current source with a slow-start, surge-free capability to protect the source. (Such a capability is required to avoid damaging or destroying the electrically fragile laser device.) The heart of the device is the National Semiconductor LM317L, an adjustable 3-terminal positive voltage source capable of supplying 100 mA over a 1.2 to 37 volt output range. The output voltage of the circuit is dependent upon the resistors as

$$V_{OUT} = V_{REF} (1 + R_2/R_1 + I_{ADJ}R_2). \quad (2.5)$$

where  $V_{REF}$  equals 1.25 volts. The adjustment current  $I_{ADJ}$  is around 100  $\mu$ A and can usually be neglected. This equation can therefore be simplified to give

$$V_{OUT} = V_{REF} (1 + R_2/R_1) \quad (2.6)$$

The slow-start portion of the circuit is the capacitor,  $C_1$ , that is charged via resistors  $R_1$  and  $R_3$ . The incorporation of capacitor  $C_1$  also acts to improve ripple

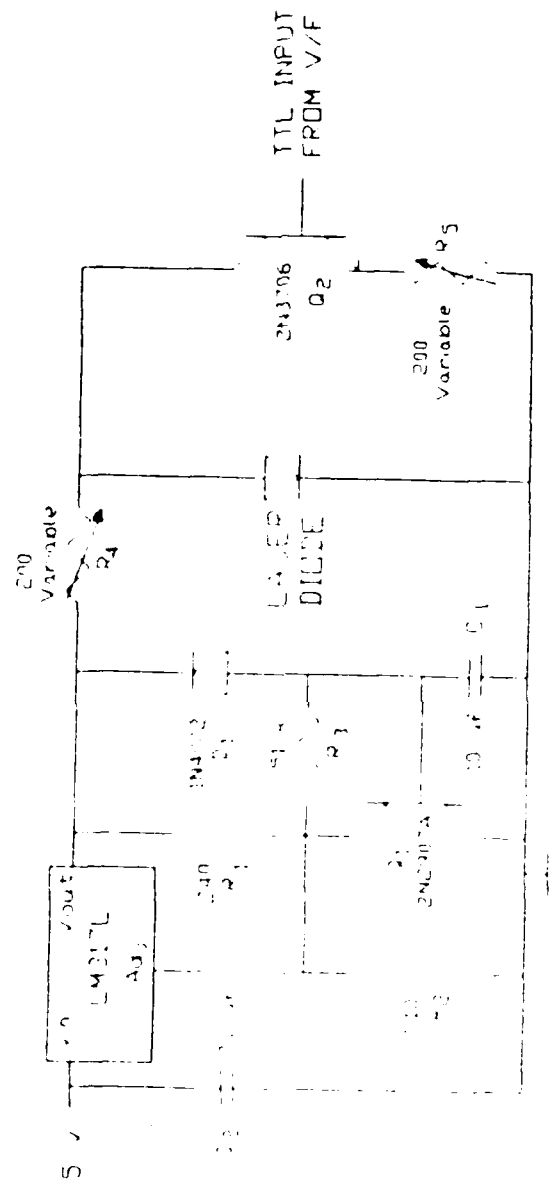


Figure 2.7 Slow start Laser diode driver circuit

reduction and noise. As  $C_1$  is charging and developing more than 0.6 volts across resistor  $R_3$ , the 2N2907A pnp transistor shunts the current from resistor  $R_2$ . Once the capacitor charges,  $Q_1$  stops conducting and the supply voltage has reached its maximum. The equation for the charging time constant is given by the following

$$t = (R_1 + R_3) * C_1 \quad (2.7)$$

In this circuit, the delay time constant is approximately 0.5 seconds. The addition of a protection diode  $D_1$  is recommended to give capacitor  $C_1$  a discharge path to ground at shut off to avoid damaging the regulator. [Ref. 9, 10]

The variable resistor  $R_4$  is used to set the operating current to the transmitter subsection (in this case  $I_{MAX}$  of the laser diode). It is recommended that another resistor can be inserted in series with variable resistor to limit  $I_{MAX}$  into the diode laser for protection of the diode. This resistor was not incorporated in the thesis because of the need to be able to switch between different sources and their differing threshold and maximum currents.

The transmitter subsection consists of the diode laser source and a 2N3706 npn transistor,  $Q_2$ . The base of  $Q_2$  is modulated by the output of the voltage-to-frequency circuit of Figure 2.6 and, when turned on, shunts a portion of the maximum current away from the diode laser through the variable resistor  $R_5$ . By adjusting  $R_5$  the amount of current shunted is enough to take the source current below threshold and as

mentioned before essentially remove the signal at the receiver.

### c. Driver Comparisons and Results

The two drivers discussed in the last sections both fit the requirements as outlined. However the slow start driver requires 18.6 mW less than the Sharp circuit and an increase of power over Gibson's original system of only 7 mW. Table III lists the power requirements of the original system along with the that of the two driver circuits. The power requirements listed range from the maximum to minimum test signals expected, that is 10 to 1 KHz.

TABLE 3  
POWER CONSUMPTION COMPARISON IN MILLIWATTS

<u>Original System</u>		
Max	-	34.6
Min	-	24.7
<u>Original System Plus Sharp Driver</u>		
Max	-	60.2
Min	-	47.0
<u>Original System Plus Slow Start Driver</u>		
Max	-	41.6
Min	-	40.3

The bandwidth of both systems, the Sharp and slow start, are limited to the bandwidth of the shunting transistor ( $Q_2$ ). In this case the 2N3706 npn transistor, which has a bandwidth of 100 MHz, was used. The actual bandwidth that the system was able to transmit without distortion was

approximately 2 MHz. For the 10 KHz transmission rates associated with this system, the bandwidth available is quite sufficient. In order to expand the system and exploit the higher bandwidth capabilities of the optoelectronics, the transistor could easily be replaced with one of greater bandwidth.

#### E. MICROPROCESSOR CONTROL AND CIRCUIT

The microprocessor that is to be used in this system is the NSC800 and is an 8-bit microprocessor chip that functions as the central processing unit (CPU) [Ref. 11]. The other main control chip utilized is the MM58167 Microprocessor Real Time Clock (RTC). Both of these low power compatible ICs are manufactured by National Semiconductor [Ref. 12]. The CPU, RTC and their related circuitry (Figure 2.8) will be addressed in the following sections.

##### 1. NSC800 Microprocessor

The NSC800 microprocessor operates using a multiplexed data and address bus structure on lines AD0 through AD7 for a reduced chip footprint. The reduced real estate is one of many advantages the NSC800; this frees pins for other input/output computational functions. Another advantage is the full line of compatible CMOS components that are available to make a complete low power system design [Ref. 11]. A reason for choosing this particular microprocessor was that it operates at a relatively low power consumption of 125 mA at

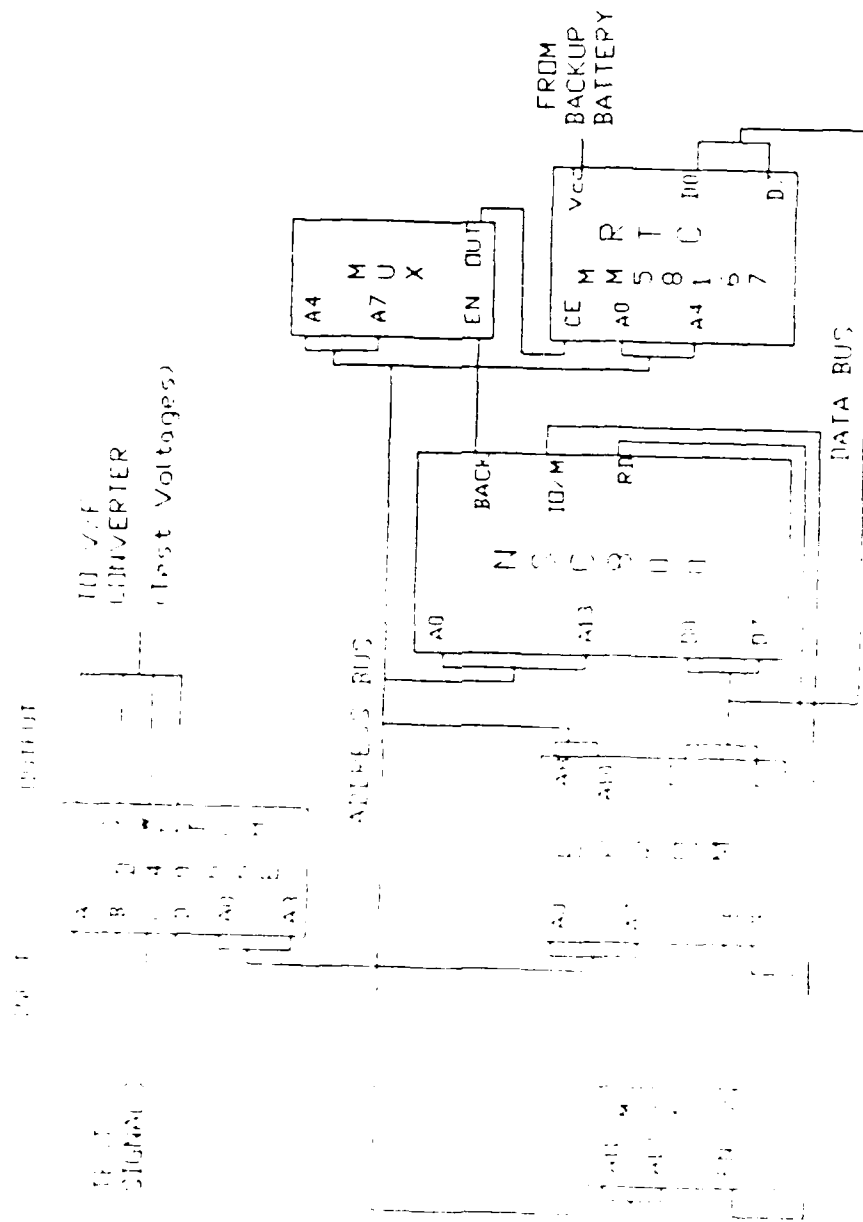


Figure 2.8 KENWOOD Microprocessor Circuity

2.5 MHz and, more importantly, it has an on-chip POWER SAVE (PS) function [Ref. 13]. This active low signal is sampled at the end of each current instruction cycle and, when asserted low, stops execution of the microprocessor at the end of the current instruction. Additionally the NSC800 has greater flexibility in its programming in that it can be programmed using the Z80 or 8080 assembly languages. [Ref. 11]

## 2. MM58167 Microprocessor Real Time Clock (RTC)

The MM58167 is a low threshold metal gate CMOS circuit that functions as a real time clock in bus-oriented microprocessor-based systems. The RTC has 56 bits of on-chip memory to compare the real time counter to the RAM data and uses less than 15 mW of power in the normal operating mode. It also has an internal twenty-four hour clock and a four year calendar that operate from its time base of 32,768 Hz using an external 32 KHz crystal oscillator circuit. The resolution of the clock counters is milliseconds and other features with this chip include a power down mode. The POWER DOWN (PD) input pin is basically an extra chip select. Asserting this pin low tells the MM58167 to go to sleep by tri-stating all inputs and outputs except for the STANDBY INTERRUPT (SI). [Ref. 12, 13] When PD is at logical zero the device will not respond to any external signals but will maintain its internal clock time keeping and assert SI low when so programmed. The low SI signal is used as the input to the POWER SAVE circuitry mentioned in the NSC800 section above; this state is achieved

when the clock reaches a preset alarm time. Conversely the SI pin is deactivated and the save power signal is removed from the PS line at the next time set in the clock memory. In the power-down mode the clock circuit draws less than 2mA of current thereby allowing considerable power consumption savings between data readings.

### 3. Controller Circuit

The MM58167 RTC, NSC800 microprocessor, and associated circuitry were chosen because of the power save and power down modes. These power down or sleep modes are the times between the voltage readings, in this case fifteen minute intervals. Since the aim of this project is to ultimately deploy this system in water up to 1000 meters deep, access to the circuit will be limited at best. Therefore, the ability to conserve battery power and increase system longevity was a primary concern and was the driving factor when designing the controller system. Basically the NSC800 controls the length of time and the order of the test voltages through the program located on an MM2764 Erasable Programmable Read Only Memory (EPROM) chip. These test voltages in turn are individually applied to the V/F converter subsystem and transmitted by the laser source. Once the end of the test program is reached, the EPROM program signals for a STANDBY INTERRUPT to be output by the RTC. The SI pin when asserted low will shut down the 5 volt power bus to the NSC800 and the rest of the system circuitry through the power MOS FETs used as switches

(Figure 2.9). During this time the RTC will be drawing power from the backup battery. In other words, the system goes into the sleep mode at the end of the test voltage routine. The design of the system is such that the entire system will be shut down (zero voltage applied to the power bus) during these sleep modes thereby increasing the total system power savings.

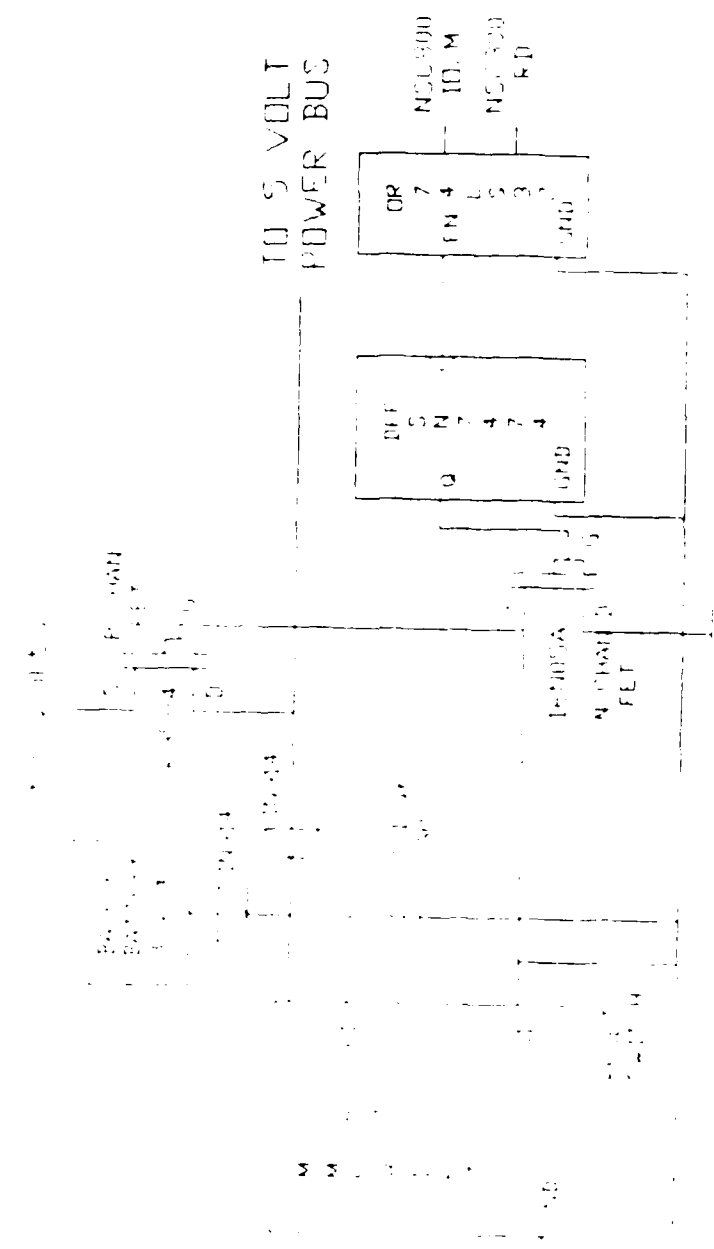


Figure 2.9 Real Time Clock Power and Sleep Circuitry

### III. TEST AND EVALUATION

Laboratory test and evaluation of the system were conducted along two tracks. The first was to determine the transmission distance of the system using the diode laser. The second was to ascertain the maximum frequency that the system was capable of modulating.

#### A. TRANSMISSION DISTANCE IMPROVEMENT

Characterization of the system over the 10 KHz to 1 KHz range was accomplished in the laboratory. The power for the setup was supplied by two batteries, 12 and 6 volts, connected in series to provide power to the 15 volt regulator and another 6 volt battery for the 5 volt regulator. These regulators provided the power to the circuitry discussed earlier in this paper. The input test voltage for the voltage-to-frequency converter was provided by a Hewlett Packard constant voltage source at or below one volt. This voltage is the simulated battery source that once frequency converted, modulates the diode laser. The output of the source was coupled into 10,898 meters of single mode fiber using an elastomeric splice. The other end of the fiber was then connected through another elastomeric splice to a Photodyne Model 19XT Automatic Attenuator capable of up to 70 dB of attenuation at 1300 nm. The 19XT was used here to

simulate another 20 Km of single mode fiber. The output of the 19XT was then fed to the Photodyne Model 1600XP Waveform Analyzer containing a Germanium avalanche photodiode detector (APD). This analyzer can detect wavelengths from 800 to 1600 nanometers and power levels as low as -40 dB. The 1600XP APD detects and converts the light energy from the fiber into electrical energy and this output signal correlates directly to the signal carried on the fiber. To determine the maximum frequency that the system could transmit the input waveform was applied directly to the modulating transistor ( $Q_2$ ) and the output of the 1600XP APD receiver was measured with a dual trace oscilloscope.

Initially the 19XT attenuator was set to 15 dB; this in combination with the nearly 11 Km of spooled single mode fiber gives a total simulated transmission distance of 41 Km. Figures 3.1 through 3.3 show photographs of the transmitted signal on the top trace and the received signal on the bottom trace after the 41 Km trip. Since each frequency received represents one of the test voltages the system can transmit, Figure 3.1 is a picture of a 10 KHz signal which corresponds to one volt frequency converted by the V/F circuit. Figures 3.2 and 3.3 show some of the lower voltages that the system is capable of frequency converting and transmitting. The 512 and 700 Hz signals of Figures 3.2 and 3.3, correspond to 0.051 and 0.07 volts respectively. The attenuation of the 19XT attenuator was increased to find the maximum amount of

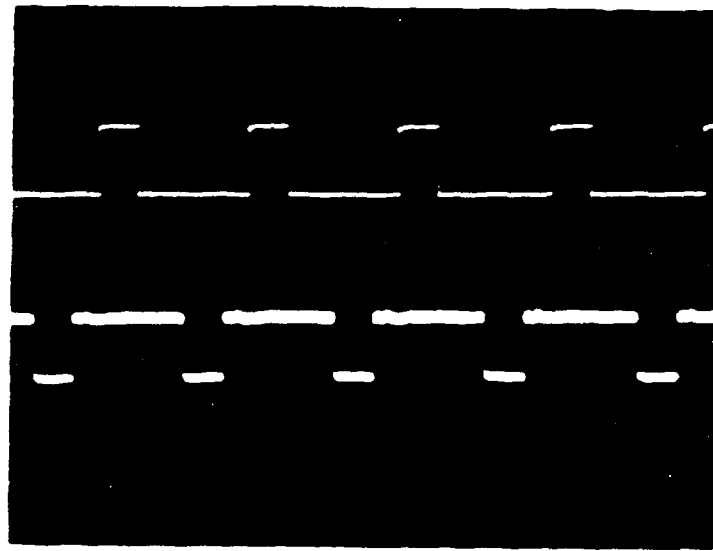


Figure 3.1 Top Trace, 10 KHz Transmitted Signal, Bottom, Received Signal (Top 2v/Div, Bottom 50mv/Div @ 50 usec/Div)

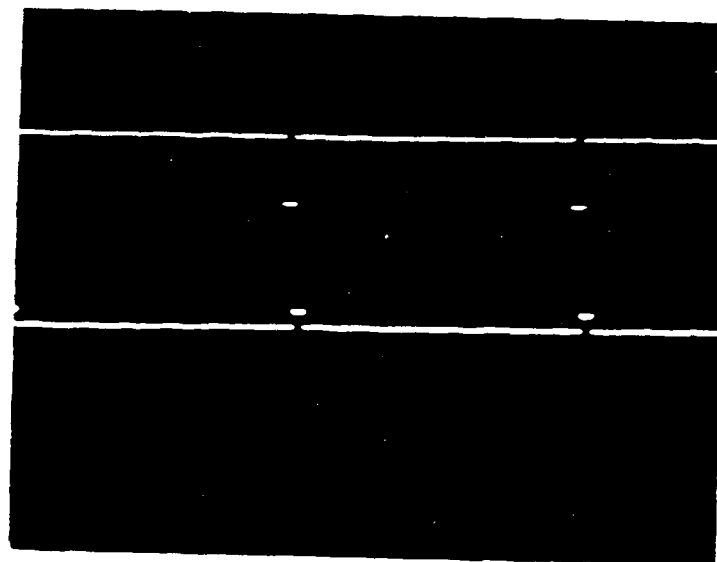


Figure 3.2 Top Trace, 512 Hz Transmitted Signal, Bottom, Received Signal (Top 2v Div, Bottom 0.5v/Div @ 0.5 msec Div)

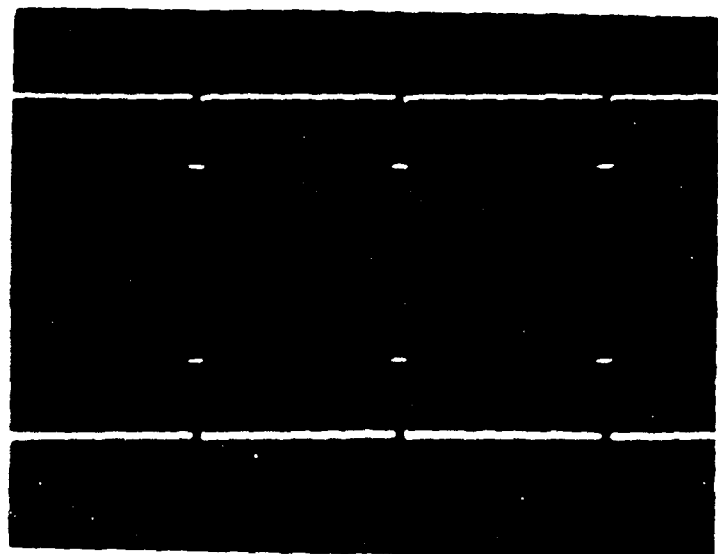


Figure 3.3 Top Trace, 700 Hz Transmitted Signal, Bottom Received Signal (Top 2v/Div, Bottom 0.1v/Div @ 0.5 msec/Div)

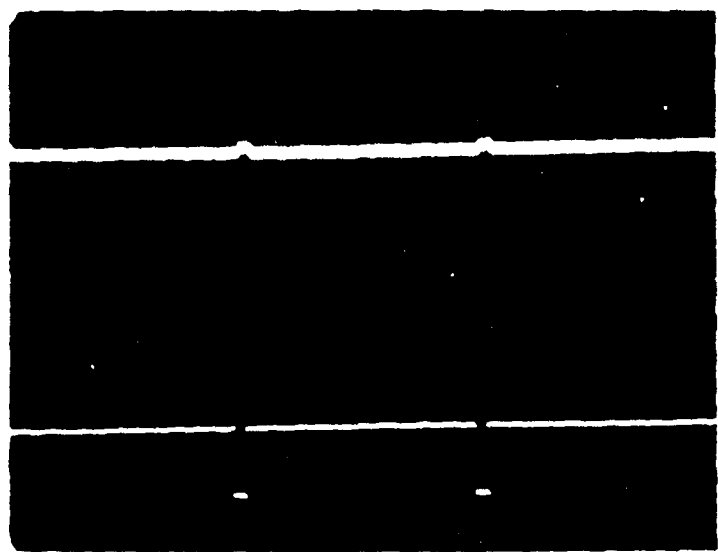


Figure 3.4 Top Trace, 280 Hz Transmitted Signal, Bottom, Received Signal After 71 Km (Top 2v/Div, Bottom 20mv/Div @ 1 usec/Div, 1600XP Set to 100mV Out/1 uW Input)

simulated fiber loss at which the received signal could still be detectable. The photographs of Figure 3.4 show a 0.023 volt (280 Hz) signal for an 19XT attenuation of 30 dB or 60 simulated Km for a total simulated fiber distance of 71 Km. The distance of 71 kilometers is the maximum distance the system could transmit using the 1600XP as its detector.

#### B. TRANSMISSION BANDWIDTH

For frequencies beyond the capabilities of the LM331 V/F circuit, that is frequencies above 10 KHz, the V/F circuit was disconnected and the shunting transistor (Q2) was directly modulated by a Wavetek 270 Programmable Function Generator. This model is capable of generating frequencies up to 12 MHz. Figures 3.5 through 3.10 show the two signals at five different frequencies from 100 KHz to 12 MHz. The need for a higher frequency generator was not required because the capacitive effects of the current producing circuit limited the bandwidth to approximately 2 MHz as mentioned in Chapter II.

In the first four photographs (Figures 3.5 through 3.8) the received signals were transmitted through the actual fiber and an additional simulated 40 Km of fiber. The receiver signal is still very recognizable although the capacitive ripples are evident. The photographs of Figures 3.9 and 3.10 are at the same frequency of 12 MHz and the signal was transmitted only through the 10,898 meters of fiber.

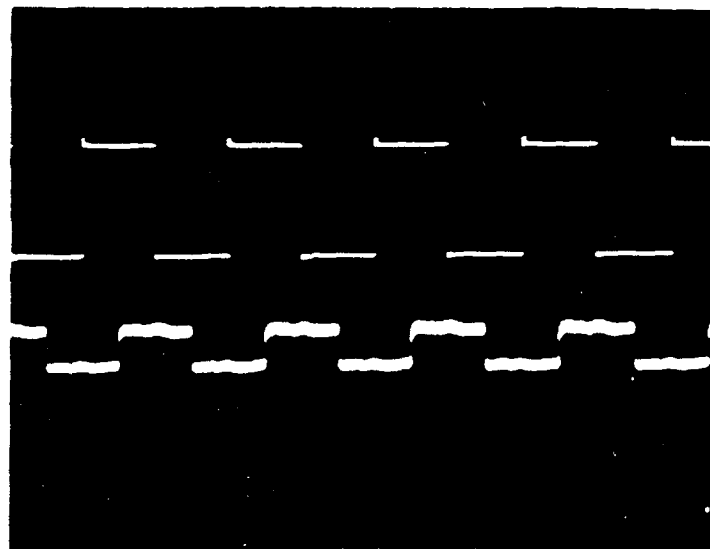


Figure 3.5 Top Trace, 100 KHz Transmitted Signal, Bottom, Received Signal Through 10898 m Fiber (Top 2v/Div, Bottom 50mV/Div @ 5 usec/Div)



Figure 3.6 Top Trace, 150 KHz Transmitted Signal Bottom, Received Signal Through 10898 m Fiber (Top 1v/Div, Bottom 10mV/Div @ 2 usec/Div)

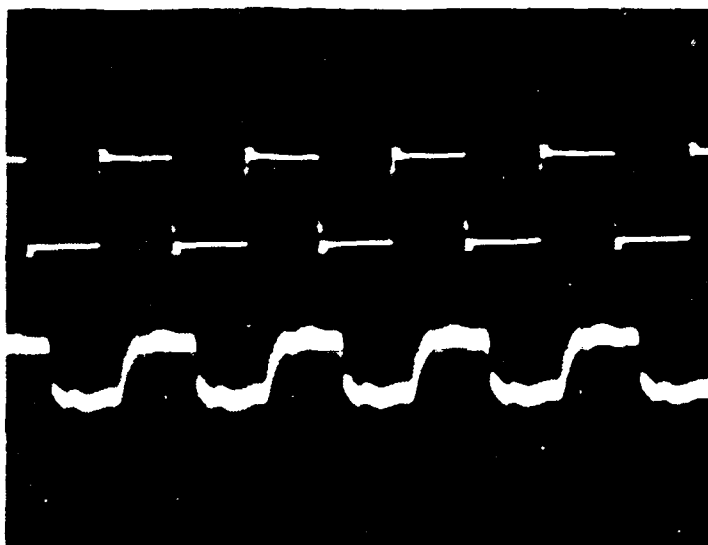


Figure 3.7 Top Trace, 500 KHz Transmitted Signal, Bottom Received Signal Through 10898 m Fiber (Top 2v/Div, Bottom 20mV/Div @ 1 usec/Div)

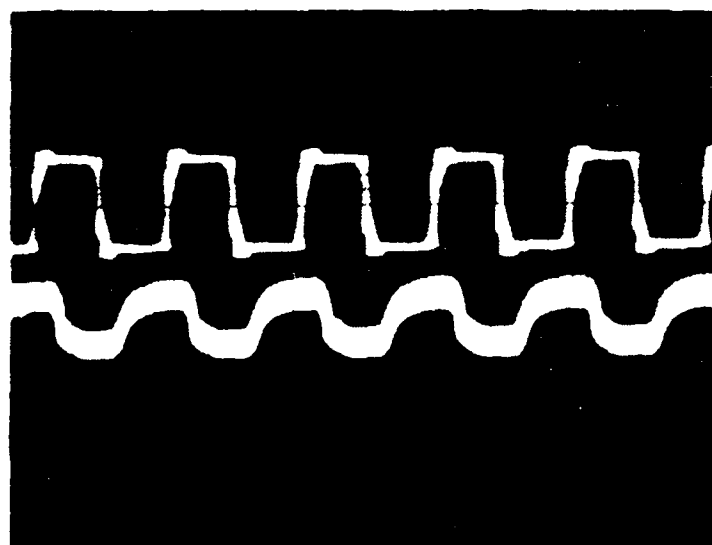


Figure 3.8 Top Trace, 1.1 MHz Transmitted Signal, Bottom Received Signal Through 10898 m Fiber (Top 2v/Div, Bottom 10mV/Div @ 0.5 usec Div)

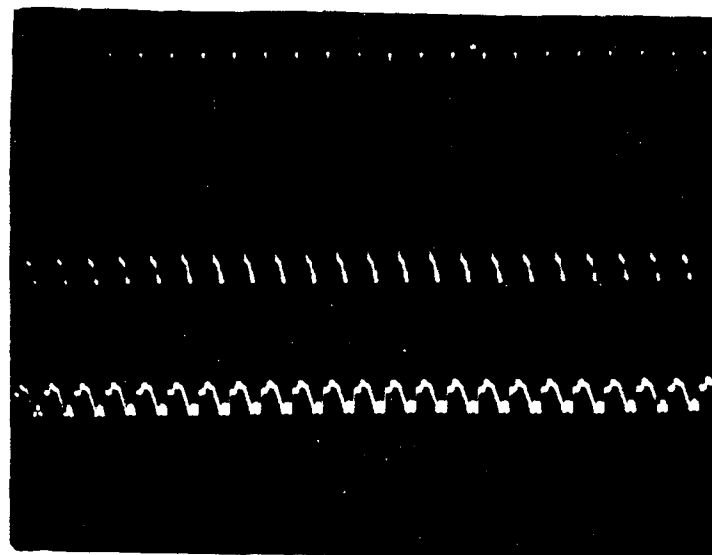


Figure 3.9 Top Trace, 12 MHz Transmitted Signal, Bottom, Received Signal Through 10898 m Fiber (Top 0.5v/Div, Bottom .05v/Div @ 0.2 usec/Div)

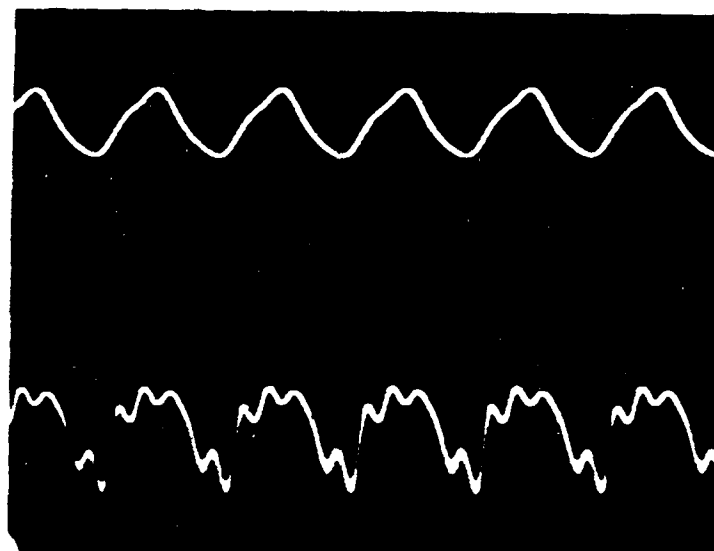


Figure 3.10 Top Trace, 12 MHz Transmitted Signal, Bottom, Received Signal Through 10898 m Fiber (Top 2v/Div, Bottom 50mv/Div @ 0.55 usec/Div, and 10X Sweep Magnification)

#### IV. CONCLUSIONS AND RECOMMENDATIONS

The modifications to the original seawater battery transmission system met and exceeded all the design criteria. The improvement in data transmission distances was greater than 69 kilometers. This increase in the distance did not come at the expense of much greater power requirements. In fact the power necessary to operate the laser diode was at worst case only 15.6 milliwatts more than the original system. The diode laser and its driver circuitry were added to Gibson's original deployable circuit board. Therefore there is no need to modify the deployment buoy.

The accuracy of the original LM331 voltage-to-frequency chip and the associated circuitry was good, but to deploy such a system, accuracy is critical. Therefore another option should be investigated. Recently Linear Technology Corporation in their latest applications book [Ref. 14] devoted an entire section to their new of state of the art voltage-to-frequency IC chips and related circuitry. These circuits have bandwidths from 1 Hz to 100 MHz and some are designed to work with 1.5 volt batteries and very small amounts of power. This change would improve the system's accuracy and at the same time make the deployed system overall more energy efficient.

## APPENDIX

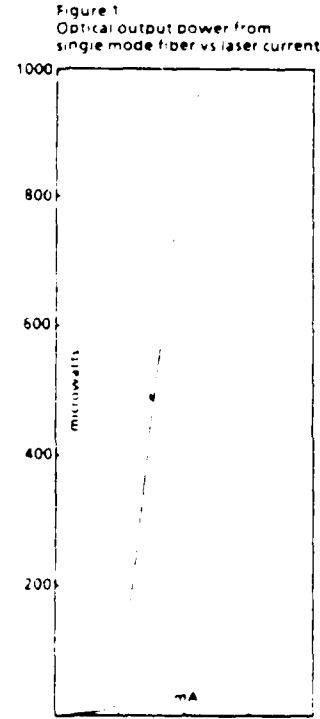
### LASERTRON DIODE LASER SPECIFICATION SHEETS (FROM REFERENCE 15)



## QLM-1300-SM-BH 1300nm Laser Module with single mode fiber

### Features:

- Advanced GaInAsP/InP laser structure
- Single mode (monomode) fiber pigtail:  $P > 0.5$  mW
- High speed modulation capability: data rate  $> 500$  Mb/s
- High performance GaInAs monitor detector
- Rugged, hermetic 14-pin dual in-line construction
- Narrow emission spectrum:  $< 3$  nm
- Reliable, high temperature operation:  $T > 50^\circ\text{C}$ .



### Description:

This module includes an efficient, low threshold laser of GaInAsP/InP buried hetero-structure geometry with thermoelectric cooler, thermistor and GaInAs InP monitor detector. High output coupling is achieved using tapered and lensed single mode Corning, ITT, GEC or Sumitomo fiber with typical peak core power in the range of 0.3 to 0.6 dBm. Special internal GaAs MESFET hybrid driver circuits are available for operation at data rates up to 700 Mb/s. Standard modules have relatively narrow emission spectra and are suitable for high data transmission applications over distances in excess of 30km when used with the Lasertron QDF pinFET receiver modules. Modules operating at other wavelengths between 1180 and 1350 nm or with special packaging are also available.

### Specifications (25°C)

	MIN	TYP	MAX
Emission wavelength (nm)	1280	1300	1320
Spectral width (nm) $\ll 500$ Mb/s)	—	2	3
Fiber coupled power (mW)	0.5	0.7	1.0
Threshold current (mA)	—	20	40
Drive current (mA for 0.5 mW)	20	40	50
Optical rise/fall time (nsec)	0.3	0.5	0.7
Operating temperature ( $^\circ\text{C}$ )	-20	—	50
Storage temperature ( $^\circ\text{C}$ )	-40	—	65
Forward voltage at full power (V)	1.4	1.5	1.8
Monitor photoreponse (mA/mW)	0.1	0.2	0.5
Monitor dark current ( $\mu\text{A}$ at $-5\text{ V}$ )	—	0.1	0.5
Monitor risetime (nsec at $-5\text{ V}$ )	—	—	1.0
Cooler current (A, $50^\circ\text{C}$ ambient)	—	—	0.5
Thermistor resistance (kOhms)	9	10	11
Thermistor temperature coefficient ( $^\circ\text{C}^{-1}$ )	—	-4	—

Figure 2  
Forward current  
vs. bias voltage.

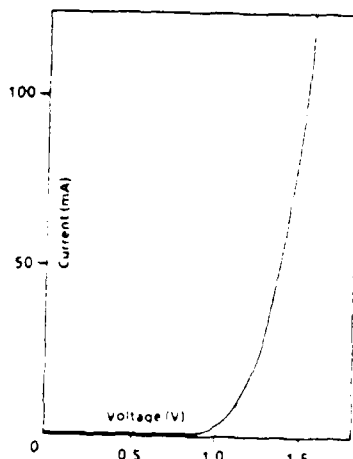


Figure 3  
Typical emission spectrum  
of optical output from fiber

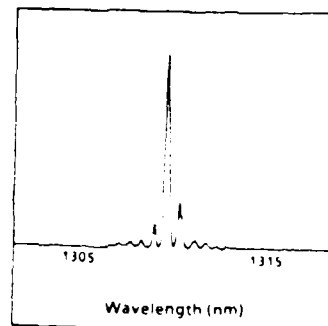
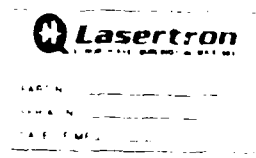
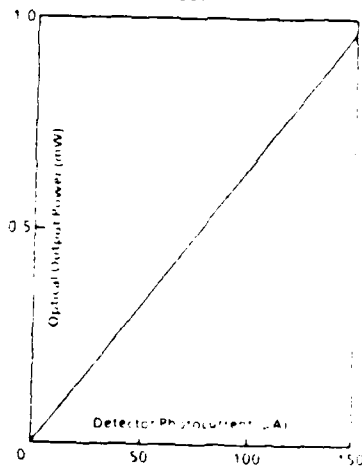


Figure 4  
Monitor detector photocurrent  
vs optical output power



ANSWER: **1. The following are the main features of the new system:**

**Q Lasertron**

11 North Avenue, Boston, Massachusetts 01813  
Telephone 617-272-5462 TWX 710-332-8926 Telex 1100-BUS



## LIST OF REFERENCES

1. Koo, Y., A Seawater Battery Monitor with Fiber Optic Remote Data Acquisition Capability, MSEE Thesis, Naval Postgraduate School, Monterey, CA, December 1985.
2. Gibson, Elton Ray, Jr, LT/USN, An Underwater Seawater Battery Monitor and Telemetry Recording System, MSEE Thesis, Naval Postgraduate School, Monterey, CA, December 1986.
3. Personick, S.E., FIBER OPTICS, Technology and Applications, (Plenum Press, New York), 1985.
4. Powers, John P., An Introduction to Fiber Optic Systems, Class Notes, Naval Postgraduate School, Monterey, CA, Spring 1986.
5. Kressel, H. and Butler, J.K., Semiconductor Lasers and Heterojunction LEDs, (Academic Press, New York), 1977.
6. Agrawal, G.P. and Dujta, N.K., Long-Wavelength Semiconductor Lasers, (Van Nostrand Reinhold Company, New York), 1986.
7. Wilkins, G., Nakagawa, A., Kamikawa, N., Design and Performance of an Undersea, Single-Fiber Multi-repeater, Full Duplex, Electro-Optical Data Link, International Telemetry Conference, San Diego, CA, October 1981.
8. Sharp Laser Diode Company, Laser Diode Handbook, 1987.
9. Mitch, John, Slow Start Circuit For Laser Diodes, Tektronics Inc., May 1987.
10. Linear Data Book, National Semiconductor Corporation, Santa Clara, CA, 1986.
11. National Semiconductor Corporation, NSC800 Microprocessor Family Handbook, Santa Clara, CA, pp 3.1 - 3.3, October 1981.
12. National Semiconductor Corporation, MM58167A Microprocessor Real Time Clock Data Sheet, Santa Clara, CA, pp 3.11 - 3.18, February 1984.

13. Davidson, Lyal B., LCDR/USN, Design And Testing of a Optical Fiber Cable Bit Error Logger, MSEE Thesis, Naval Postgraduate School, Monterey, CA, December 1984.
14. Linear Technology Corporation, Linear Applications Handbook, Milpitas, CA, pp AN 14.1-20, October 1986.
15. Lasertron Incorporated, QLM-1300-SM-BH, 1300nm Laser Module with Single Mode Fiber, Specifications, 15 July 1985.

## BIBLIOGRAPHY

1. Powers, John P., "A Fiber Optic Digital Uplink For Ocean Floor Experimentation", Proceedings of SPIE - The International Society for Optical Engineering, v. 506, pp. 82-87, 1984.
2. Arecchi, F.T. and Schulz-Dubois, E.O., Editors, "Semiconductor Lasers: Devices", Laser Handbook, (North-Holland Publishing Company, New York), pp 444-496, 1972.
3. Arecchi, F.T. and Schulz-Dubois, E.O., Editors, "Design Of Solid-State Lasers", Laser Handbook, (North-Holland Publishing Company, New York), pp 497-528, 1972.
4. McCartney, D.J., Payne, D.B., "Monomode Optical Fibre Splicing", Proceedings of SPIE - The International Society for Optical Engineering, v. 500, pp. 37-43, 1984.
5. Okoshi, T., Optical Fibers, (Academic Press, New York), 1982.

INITIAL DISTRIBUTION LIST

	No. Copies
1. Library, Code 0142 Naval Postgraduate School Monterey, California 93943-5002	2
2. Defense Technical Information Center Cameron Station Alexandria, Virginia 22304-6145	2
3. Department Chairman, Code 62 Department of Electrical and Computer Engineering Naval Postgraduate School Monterey, California 93943-5000	1
4. Professor John Powers, Code 62Po Department of Electrical and Computer Engineering Naval Postgraduate School Monterey, California 93943-5000	5
5. Professor S. Michael, Code 62Mi Department of Electrical and Computer Engineering Naval Postgraduate School Monterey, California 93943-5000	1
6. Professor C. R. Dunlap, Code 68Du Department of Physics Naval Postgraduate School Monterey, California 93943-5000	1
7. Commanding Officer Naval Oceanographic Systems Center Attn Mr. William Ehlers San Diego, CA. 92152-5000	2
8. Lieutenant John G. Gallagher, USN 4117 Whitfield Avenue Fort Worth, Texas 76109	2

END

DATE  
FILMED

5- 88

DTIC